Structure and Characterization of $KSc(BH_4)_4$

Radovan Černý,*,† Dorthe B. Ravnsbæk,‡ Godwin Severa,§ Yaroslav Filinchuk,|| Vincenza D' Anna,⊥ Hans Hagemann,⊥ Dörthe Haase,# Jørgen Skibsted,‡ Craig M. Jensen,*,§ and Torben R. Jensen*,‡

Laboratory of Crystallography, University of Geneva, 1211 Geneva, Switzerland, Center for Materials Crystallography, Interdisciplinary Nanoscience Center (iNANO) and Department of Chemistry, University of Aarhus, Langelandsgade 140, DK-8000 Århus C, Denmark, Department of Chemistry, University of Hawaii at Manoa, 2545 The McCarthy Mall, Honolulu, Hawaii 96822-227, Swiss-Norwegian Beamlines at ESRF, BP-220, 38043 Grenoble, France, Department of Physical Chemistry, University of Geneva, 1211 Geneva, Switzerland, and MAX-lab, Lund University, S-22100 Lund, Sweden

Received: July 7, 2010; Revised Manuscript Received: September 24, 2010

A new potassium scandium borohydride, $KSc(BH_4)_4$, is presented and characterized by a combination of *in situ* synchrotron radiation powder X-ray diffraction, thermal analysis, and vibrational and NMR spectroscopy. The title compound, $KSc(BH_4)_4$, forms at ambient conditions in ball milled mixtures of potassium borohydride and $ScCl_3$ together with a new ternary chloride K_3ScCl_6, which is also structurally characterized. This indicates that the formation of $KSc(BH_4)_4$ differs from a simple metathesis reaction, and the highest scandium borohydride yield (~31 mol %) can be obtained with a reactant ratio KBH_4:$ScCl_3$ of 2:1. $KSc(BH_4)_4$ crystallizes in the orthorhombic crystal system, $a = 11.856(5)$, $b = 7.800(3)$, $c = 10.126(6)$ Å, $V = 936.4(8)$ Å^3 at RT, with the space group symmetry *Pnma*. $KSc(BH_4)_4$ has a $BaSO_4$ type structure where the BH_4 tetrahedra take the oxygen positions. Regarding the packing of cations, K^+, and complex anions, $[Sc(BH_4)_4]^-$, the structure of $KSc(BH_4)_4$ can be seen as a distorted variant of orthorhombic neptunium, Np, metal. Thermal expansion of $KSc(BH_4)_4$ in the temperature range RT to 405 K is anisotropic, and the lattice parameter *b* shows strong nonlinearity upon approaching the melting temperature. The vibrational and NMR spectra are consistent with the structural model, and previous investigations of the related compounds $ASc(BH_4)_4$ with A = Li, Na. $KSc(BH_4)_4$ is stable from RT up to ~405 K, where the compound melts and then releases hydrogen in two rapid steps approximately at 460−500 K and 510−590 K. The hydrogen release involves the formation of KBH_4, which reacts with K_3ScCl_6 and forms a solid solution, $K(BH_4)_{1-x}Cl_x$. The ternary potassium scandium chloride K_3ScCl_6 observed in all samples has a monoclinic structure at room temperature, $P2_1/a$, $a = 12.729(3)$, $b = 7.367(2)$, $c = 12.825(3)$ Å, $\beta = 109.22(2)°$, $V = 1135.6(4)$ Å^3, which is isostructural to K_3MoCl_6. The monoclinic polymorph transforms to cubic at 635 K, $a = 10.694$ Å (based on diffraction data measured at 769 K), which is isostructural to the high temperature phase of K_3YCl_6.

Introduction

Metal borohydrides are considered as possible hydrogen storage materials for mobile applications.[1,2] Borohydrides of alkaline and alkaline earth metals often contain large quantities of hydrogen, e.g., 18.4 wt % in $LiBH_4$. Unfortunately, decomposition temperatures are usually high and rehydrogenation only occurs under harsh conditions for this class of materials dominated by ionic interactions between the metal and complex ion $[BH_4]^-$.[3,4] The relatively stable alkaline and alkaline earth metal borohydrides form in some cases with transition metals new bimetallic phases, which may improve the thermodynamic properties.[5−8]

Metal borohydrides are known to have a rich chemistry and can also form eutectic melting mixtures as observed for the $Ca(BH_4)_2$−$LiBH_4$ system or new solids as in the $Al(BH_4)_3$−$LiBH_4$ system, i.e., $Li_4Al_3(BH_4)_{13}$.[9,10] The thermal stability of binary metal hydrides has been inversely related to the metal electronegativity (and consequently to the standard redox potential).[3] A similar relation has been postulated also for borohydrides a half-century ago,[11] based on the stability ratio theory of Sanderson,[12] and has been recently analyzed theoretically and experimentally.[13−15] This suggests that synthesis and characterization of novel metal borohydrides may be a fruitful approach to obtain more favorable thermodynamic properties and the hydrogen release temperature.

Homoleptic metal borohydrides are known to form a variety of structure types.[16] Compounds like $Al(BH_4)_3$, $Zr(BH_4)_4$,[17] $Hf(BH_4)_4$,[18] and $U(BH_4)_4$[19] form molecular compounds, whereas $Y(BH_4)_3$ forms a 3D-framework structure.[20−23] Homoleptic scandium borohydride has been many times reported as $Sc(BH_4)_3$, and a rhombohedral structural model has been predicted from energy minimization.[13] However, no experimental evidence supporting the existence of $Sc(BH_4)_3$ is reported up to now. In contrast, $Y(BH_4)_3$ is found to crystallize in two different cubic polymorphs, one at room temperature[20] and one

* Corresponding authors. E-mail: Radovan.Cerny@unige.ch (R.C.); jensen@hawaii.edu (C.M.J.); trj@chem.au.dk (T.R.J.). Phone: +41 22 379 6450 (R.C.); +1 808 956 2769 (C.M.J.); +45 8942 3894 (T.R.J.). Fax: +41 22 379 6108 (R.C.); +1 808 956 5908 (C.M.J.); +45 8619 6199 (T.R.J.).

† Laboratory of Crystallography, University of Geneva.

‡ University of Aarhus.

§ University of Hawaii at Manoa.

|| Swiss-Norwegian Beamlines at ESRF.

⊥ Department of Physical Chemistry, University of Geneva.

Lund University.

10.1021/jp106280v
Published on Web 10/25/2010

above 453 K.[22,23] On the other hand, scandium readily forms bimetallic homoleptic borohydrides based on the $[Sc(BH_4)_4]^-$ anion, e.g., with lithium, $LiSc(BH_4)_4$, and sodium, $NaSc(BH_4)_4$.[24,25] Here, we report on the synthesis, crystal structure, hydrogen desorption properties, and Raman, infrared, and NMR spectra of another scandium-based bimetallic borohydride, $KSc(BH_4)_4$.

Experimental Section

Synthesis. The preparation and manipulation of all samples were performed in an argon-filled glovebox with a circulation purifier ($p(O_2, H_2O) < 0.1$ ppm). Anhydrous scandium chloride, $ScCl_3$ (Sigma-Aldrich, 99.7%), and potassium borohydride, KBH_4 (Sigma-Aldrich, 98.5%), were combined in the molar ratios 1:2, 1:3, and 1:4 and ball milled 120 min under inert conditions (argon atmosphere) in a Fritsch Pulverisette planetary mill using 80 mL tungsten carbide steel containers using an approximately 1:35 ratio of sample to 10 mm balls.

Laboratory X-ray Powder Diffraction (PXD). All samples were initially investigated using in house powder X-ray diffraction (PXD) in order to identify the reaction products and estimate the crystallinity of the samples. PXD measurements were performed in Debye−Scherrer transmission geometry using a Stoe diffractometer equipped with a curved Ge(111) monochromator (Cu $K\alpha_1$ radiation) and curved position sensitive detector. Data were collected at room temperature (RT) between 4 and 127° 2θ with a counting time of ∼960 s per step. Air-sensitive samples were mounted in a glovebox between two Mylar films (3.6 μm thick) or in 0.4 mm glass capillaries sealed with glue.

Thermal Analysis. Simultaneous thermogravimetric analysis (TG) and differential scanning calorimetry (DSC) was performed using a Netzsch STA449C Jupiter instrument (heating rate 2 K/min, RT to 773 K) and corundum crucibles with a lid as the sample holder. The experiments were conducted in a helium (4.6 purity) atmosphere.

In Situ Time-Resolved Synchrotron Radiation Powder X-ray Diffraction (SR-PXD). One set of SR-PXD was collected on the sample 2:1 at the Swiss-Norwegian Beamlines (SNBL) at the European Synchrotron Radiation Facility (ESRF) in Grenoble, France. The sample was mounted in a glass capillary (o.d. 0.5 mm) sealed with wax, and heated from RT to 500 K at a rate of 1 K/min while synchrotron radiation powder X-ray diffraction data (SR-PXD) were collected. The temperature was controlled with the Oxford Cryostream 700+. The data were collected using a MAR345 image plate detector at a sample-to-detector distance of 250 mm and radiation with a selected wavelength of $\lambda = 0.700128$ Å. The capillary was oscillated by 60° during exposure to the X-ray beam for 60 s, followed by a readout for ∼83 s. This data set has been used for structure solution of $KSc(BH_4)_4$.

Other sets of SR-PXD data were collected on the samples 2:1, 3:1, and 4:1 at the beamline I711 or I911-5 of the synchrotron MAX II, Lund, Sweden, in the research laboratory MAX-Lab with a MAR165 CCD detector system and selected wavelengths of 1.097 or 0.9077 Å for measurements conducted at I711 and I911, respectively.[26] The CCD camera exposure time was 30 s. The sample cell was specially developed for studies of gas/solid reactions and allows high pressure and temperature to be applied.[27,28] The powdered samples were mounted in a sapphire single crystal tube (o.d. 1.09 mm, i.d. 0.79 mm) in an argon-filled glovebox ($p(O_2, H_2O) < 1$ ppm). The sample holder was sealed inside the glovebox. A flexible rubber balloon is sealing the open end of the sample holder (connected to both ends of the sapphire capillary holding the sample) so that the internal total pressure constantly equals the atmospheric pressure during the entire X-ray experiment. On the other hand, the partial pressure of hydrogen in the sample holder will increase during the X-ray experiment due to thermal decomposition of the sample. The temperature was controlled with a thermocouple placed in the sapphire tube 1 mm from the sample. The samples were typically heated from RT to 773 K with a selected heating rate of 5−10 K/min. These data sets have been used for the decomposition analysis.

The raw images were transformed to 2D powder diffraction patterns using the FIT2D program,[29] which was also used to remove diffraction spots from the single crystal sapphire tube used as a sample holder.

Structure Solution and Refinement. The seven observed peaks of $KSc(BH_4)_4$, identified as diffraction peaks that simultaneously vanish at ∼405 K, were indexed with DICVOL04[30] in the orthorhombic lattice with $a = 11.856(5)$, $b = 7.800(3)$, $c = 10.126(6)$ Å, and $V = 936.4(8)$ Å^3 at RT. Initially, systematic extinctions were not easily recognized, leading to several possible space groups. In the next iteration, space group *Pnma* was selected and the structure was solved with the direct space method program FOX,[31] and refined with the Rietveld method using the TOPAS program.[32] The symmetry of the refined structure has been checked with the routine ADDSYM in the program PLATON,[33] and the space group *Pnma* has been confirmed. The resulting structure containing one K atom (position 4*c*), one Sc atom (position 4*c*), and three BH_4 groups (two boron atoms at position 4*c* and one at 8*d*) in the asymmetric unit was refined by the Rietveld method. The structure was solved and refined with the BH_4 groups as semirigid ideal tetrahedra with one common refined B−H distance. For two boron atoms situated on the mirror plane symmetry, the BH_4 tetrahedra were allowed only to translate and to rotate following the mirror plane symmetry. Three antibump distance restraints were needed to stabilize the shape of the complex anion $[Sc(BH_4)_4]^-$ in the structure: Sc−H 2.3, B−B 4.0, and K−B 3.7 Å. An overall displacement parameter has been refined isotropically. The uncertainties of crystallographic coordinates of hydrogen atoms were not available from the least-squares matrix, and were estimated by the bootstrap method.[34] The agreement factors are as follows: R_{wp} (not corrected for background) = 3.33%, R_{wp} (corrected for background) = 7.56%, $\chi^2 = 93$, R_{Bragg} ($KSc(BH_4)_4$) = 1.50%, and R_{Bragg} (K_3ScCl_6) = 0.60%. The high value of χ^2 reflects mainly the extremely high counting statistics of the powder diffraction data obtained from modern 2D detectors.

Raman and Infrared (IR) Spectroscopy. Raman spectra were obtained on the sample 2:1 using a Kaiser Holospec Monochromator in conjunction with a liquid nitrogen cooled CCD camera. Spectra were excited using the laser wavelength 488 nm with a typical laser power of 50 mW. The spectral resolution of the Raman spectra is about 3 cm^{-1}. The samples were sealed in melting point capillaries.

IR spectra were measured on the sample 2:1 using a Biorad Excalibur instrument equipped with a Specac low temperature Golden Gate diamond ATR system. The spectral resolution was set to 1 or 2 cm^{-1} for the different experiments. Samples were loaded in the glovebox in the ATR system.

MAS NMR Spectroscopy. Solid-state ^{11}B MAS NMR spectra for the ball milled sample of KBH_4-ScCl_3 (2:1) were recorded on a Varian Unity-INOVA-300 (7.05 T) spectrometer using home-built CP/MAS NMR probes for 5 mm outer diameter (o.d.) rotors. The NMR experiments were performed at ambient temperatures using airtight end-capped zirconia

TABLE 1: Comparison of the Sample Composition after Ball Milling (BM), Total H_2 Content, and the Observed TGA Mass Loss for the Three Investigated Samples

$ScCl_3$:KBH_4	1:2		1:3		1:4	
composition after BM	mol %	wt %	mol %	wt %	mol %	wt %
$KSc(BH_4)_4$	31	18	15	17	3	4
K_3ScCl_6	51	78	19	55	13	49
KBH_4	18	4	66	28	84	47
total H_2 content	wt %		wt %		wt %	
	3.11		3.86		4.39	
observed TGA mass loss		wt %		wt %		wt %
		1.44		1.94		2.32

rotors, which were packed with the sample in the Ar-filled glovebox. The ^{11}B isotropic chemical shifts are in ppm relative to neat $F_3B \cdot O(CH_2CH_3)_2$.

Solid-state ^{45}Sc MAS NMR spectra were collected on a Varian Inova spectrometer equipped with a 3.2 mm HX CPMAS probe (Varian Chemagnetics, Ft Collins, CO) operating at 97.2 MHz. The samples were packed in 3.2 mm rotors and spun at 10 kHz. Single pulse excitation with pulse widths of 0.8 μs was used. The NMR shifts are reported with respect to aqueous $ScCl_3$.

Results and Discussion

Synthesis and Phase Analysis. The KBH_4-ScCl_3 samples all contain two sets of unidentified Bragg peaks. One of these was assigned to $KSc(BH_4)_4$, and the other was assigned to a new ternary potassium scandium chloride K_3ScCl_6, which is isostructural to K_3MoCl_6,[35] and was identified as an additional phase in all samples. The sample composition after ball milling was found by Rietveld refinement of the SR-PXD data measured at RT, and for the sample of molar ratio 2:1, the main reaction product is K_3ScCl_6 (~51 mol %). The remaining fraction of the sample is ~31 mol % $KSc(BH_4)_4$, and a smaller amount of unreacted KBH_4 corresponding to ~18 mol %. The samples with higher KBH_4 content before milling yield lower amounts of $KSc(BH_4)_4$, and the amount of K_3ScCl_6 also decreases, while the content of unreacted KBH_4 drastically increases. Thus, the 2:1 samples contain the largest fraction of the new compound $KSc(BH_4)_4$ (see Table 1). Diffraction peaks from $ScCl_3$ were not observed in any of the samples.

The PXD data shows no presence of KCl in any sample, which indicates that the reaction during the ball milling differs from the reactions observed for formation of $LiSc(BH_4)_4$[24] from $LiBH_4$ and $ScCl_3$. Instead, the reaction pathway seems to be similar to that suggested for $NaBH_4$:$ScCl_3$ mixtures, yielding $NaSc(BH_4)_4$ and Na_3ScCl_6,[25] and can in this case be described as

$$4KBH_4 + 2ScCl_3 \rightarrow KSc(BH_4)_4 + K_3ScCl_6 \qquad (1)$$

This further indicates that the optimal starting ratio between KBH_4 and $ScCl_3$ is 2:1. Reaction 1 may consist of two subreactions, i.e., possibly formation of KCl as an intermediate via a metathesis reaction, followed by fast formation of K_3ScCl_6 via an additional reaction between $ScCl_3$ and KCl.

Crystal Structure of $KSc(BH_4)_4$. The table with refined atomic positions of $KSc(BH_4)_4$ is given in the Supporting Information as Table S1, selected bond distances and angles on the $[Sc(BH_4)_4]^-$ anion are given as Table S2, and the Rietveld plot is shown as Figure S1. The table with refined atomic positions of K_3ScCl_6 is given as Table S3. The structural drawing of $KSc(BH_4)_4$ viewed approximately along the *b*-axis is shown in Figure 1. The basic building unit for the structure of $KSc(BH_4)_4$ is the borohydride complex $[BH_4]^-$, which is a regular tetrahedron. A single B−H distance of 1.148(2) Å was refined for the semirigid BH_4 tetrahedra. It compares well with those refined with single crystal X-ray diffraction data in related borohydrides such as $Mg(BH_4)_2$ (1.142 Å on average[36]) and $NaBH_4$ and its dihydrate, $NaBH_4 \cdot 2H_2O$ (1.09−1.13 Å[37]).

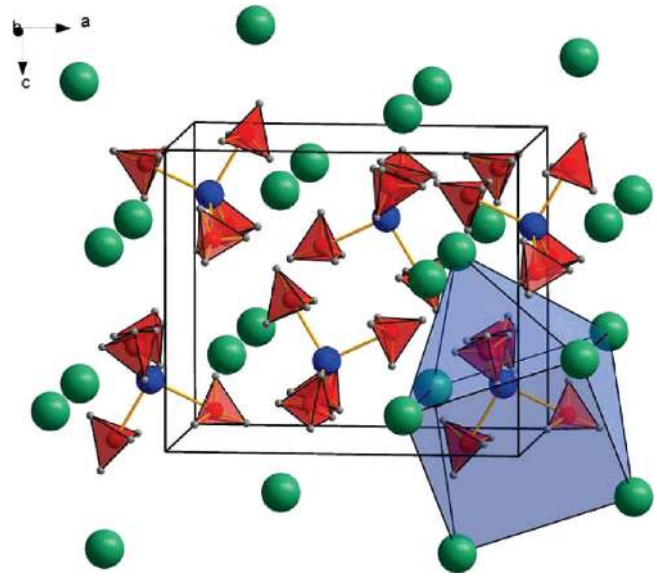

Figure 1. Crystal structure of $KSc(BH_4)_4$ (structure type $BaSO_4$) viewed approximately along the *b*-axis, showing the coordination of Sc atoms (blue) by BH_4 tetrahedra (red), K atoms in green. The side monocapped trigonal prism ScK_7 is shown in light blue.

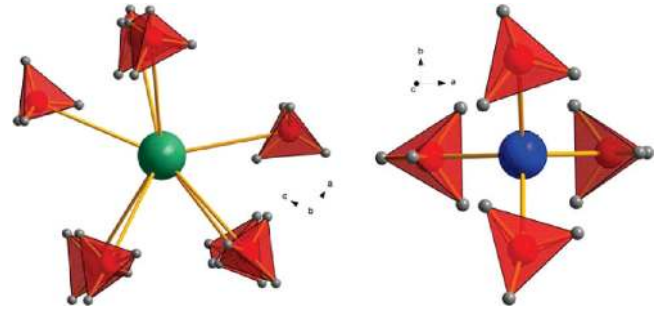

Figure 2. Coordination of K atoms (green) and Sc atoms (blue) by BH_4 tetrahedra (red) in $K(BH_4)_8$ side bicapped trigonal prism and $Sc(BH_4)_4$ tetrahedron.

The scandium atom is surrounded by four BH_4 tetrahedra (see Figure 2), forming a slightly deformed tetrahedral environment (Sc−B distances within 2.27(2)−2.38(3) Å, B−Sc−B angles within 95.5(14)−114.9(5)°). This coordination resembles (Table S2, Supporting Information) the almost ideal tetrahedral $[Sc(BH_4)_4]^-$ anion, as found by DFT optimization of the isolated $[Sc(BH_4)_4]^-$ anion, and is less deformed than the experimentally observed $[Sc(BH_4)_4]^-$ anion in $LiSc(BH_4)_4$[24] but more deformed than the same anion in $NaSc(BH_4)_4$.[25] However, the degree of the anion's deformation does not follow exactly the increasing site symmetry of its position in the crystal structure: *m* in $KSc(BH_4)_4$, 222 in $LiSc(BH_4)_4$, and *m*2*m* in $NaSc(BH_4)_4$. The Sc−B distances are very similar in all three known alkali metal (Li, Na, and K) scandium borohydrides based on the complex anion $[Sc(BH_4)_4]^-$, and compare well to those in the molecular compounds $Zr(BH_4)_4$ at 113 K[17] and $Hf(BH_4)_4$ at 110 K.[18] The

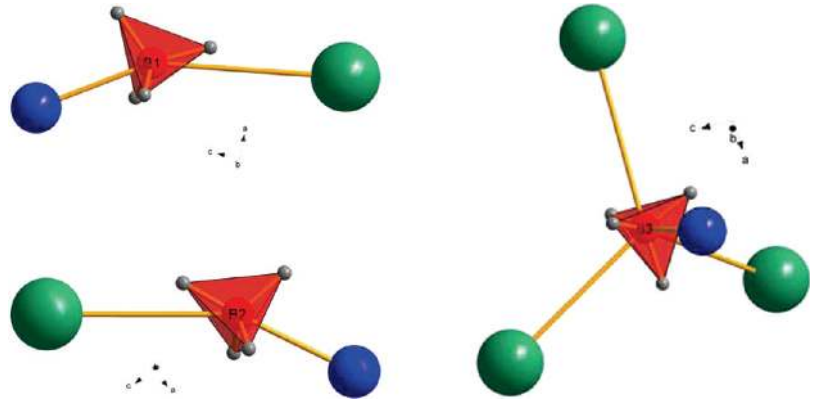

Figure 3. Coordination of B atoms (red) by Sc (blue) and Na atoms (green).

only other tetrahedral homoleptic complex anion characterized in a nonsolvated borohydride is $[Al(BH_4)_4]^-$ in $Li_4Al_3(BH_4)_{13}$[10] with shorter Al−B distances of 2.237(6) Å in agreement with a smaller ionic radius of Al^{3+}.

The potassium atom is surrounded by eight BH_4 tetrahedra (see Figure 2), forming a side bicapped trigonal prismatic coordination with K−B distances within 3.51(4)−3.95(2) Å. This coordination is rather unusual compared to the regular octahedral coordination of sodium in $NaSc(BH_4)_4$ but compares well with the distorted square antiprismatic coordination of potassium by five Cl^- and three $[BH_4]^-$ within 3.19−3.75 Å in recently discovered $KZn(BH_4)Cl_2$.[38]

The structure of $KSc(BH_4)_4$ contains three independent BH_4 tetrahedra with two different types of coordination (see Figure 3): two borohydride groups, B1 and B2, are coordinated by one scandium and one potassium atom with Sc−B−K angles of 155(1) and 154(1)°, respectively, which are closer to a linear coordination than the B1 group in $NaSc(BH_4)_4$. The third borohydride group, B3, is coordinated by one scandium and three potassium atoms in a deformed tetrahedral coordination, i.e., the metal−B3−metal angles range from 96.9(6) to 121.1(5)°. The tetrahedral coordination of a borohydride group *via* the four faces has been observed only in the hexagonal HT phase of $LiBH_4$,[39,40] in $NaZn(BH_4)_3$,[41] and in the complex cation $[(BH_4)Li_4]^{3+}$ in $Li_4Al_3(BH_4)_{13}$.[10]

The mode of BH_4 coordination by scandium and potassium atoms is determined only approximately using the structural model with pseudorigid ideal BH_4 tetrahedra, and antibump restraints. The coordination mode for the BH_4 group to scandium corresponds to the Sc···H_3B scheme; i.e., the BH_4 tetrahedron has a plane of three H-atoms oriented toward Sc. It results in a 12-fold coordination of Sc to hydrogen with Sc−H distances in the range 2.0(1)−2.4(1) Å which is closer to an ideal cuboctahedron than in $NaSc(BH_4)_4$. Contrary to that, the bonding scheme in $[Al(BH_4)_4]^-$ in $Li_4Al_3(BH_4)_{13}$[10] is bidentate, Al···H_2B, again in agreement with the smaller ionic radius of Al^{3+}. Potassium coordination by hydrogen in $KSc(BH_4)_4$ cannot be classified without ambiguities.

Raman and Infrared Spectroscopy. The vibrational spectra of $ASc(BH_4)_4$ with A = Li, Na, and K present many similarities, which appear to be characteristic for $M(BH_4)_4$ complexes with tridentate coordination of M by BH_4 tetrahedral faces (see Figures 4 and 5). The vibrational properties of neutral complexes (M = Zr, Hf, and U) have been reviewed by Marks and Kolb.[42] Table S4 in the Supporting Information summarizes the observed IR bands for the three scandium compounds and compares them with literature values for $Zr(BH_4)_4$[43] and $Hf(BH_4)_4$.[44] The strongest IR band is observed at about 1190

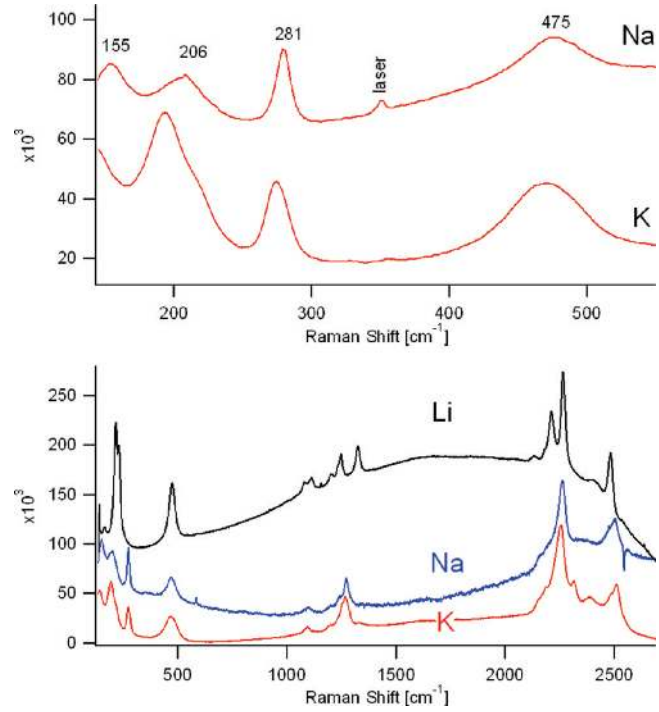

Figure 4. Raman spectra of alkali metal−scandium borohydride samples.

cm^{-1} for all three Sc compounds (Figure 5) and at 1221 and 1218 cm^{-1} for $Zr(BH_4)_4$ and $Hf(BH_4)_4$. The B−H stretching modes are split into two groups around 2480 and 2200 cm^{-1} for the Sc compounds (Figure 5). In the case of the Zr and Hf compounds, this splitting is larger (ca. 400 cm^{-1}). This difference distinguishes the $MSc(BH_4)_4$ compounds from the molecular complexes $M(BH_4)_4$ with M = Zr, Hf, U, and Np. The IR spectra of these molecular complexes present additionally a strong band at ca. 480 cm^{-1} assigned to the T_2 metal to the boron stretching mode.

Another characteristic feature is the corresponding strong Raman bands (see Figure 4) observed around 200 and 480 cm^{-1} assigned to metal to boron bending and stretching motions, respectively.

The sharp bands observed in the Raman spectra (see Figure 4) around 280 cm^{-1} correspond to the symmetrical Sc−Cl stretch of A_3ScCl_6 (A = Na and K).

NMR Spectroscopy. The ^{11}B MAS NMR spectra (Figure 6a) of the central transitions for the ball milled sample of KBH_4−$ScCl_3$ (2:1) show two separate ^{11}B resonances centered at −22.2 and −37.8 ppm, respectively. The resonance at −37.8

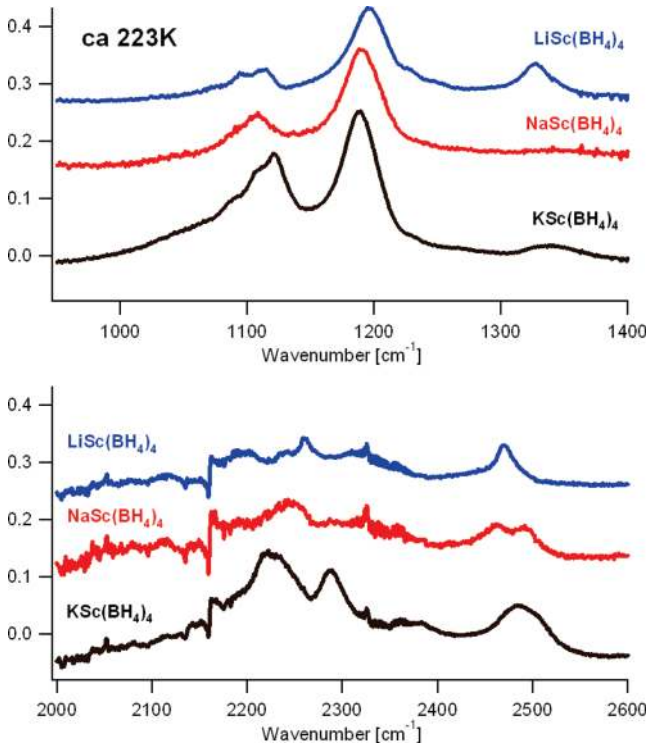

Figure 5. Infrared spectra of alkali metal−scandium borohydride samples.

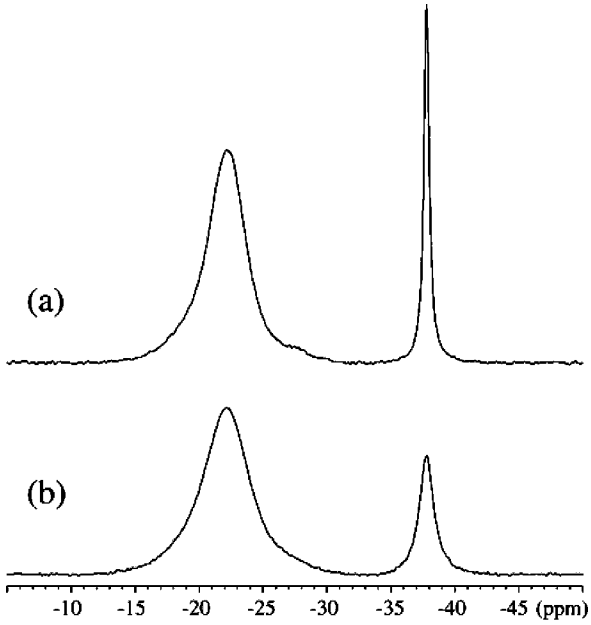

Figure 6. ^{11}B MAS NMR spectrum (7.05 T) of the ball milled KBH_4-ScCl_3 (2:1) sample recorded (a) with and (b) without ^{1}H decoupling. Both spectra employ a spinning speed of $\nu_R = 10.0$kHz, a 4 s repetition delay, and 128 scans.

ppm originates from KBH_4,[38] while the resonance at −22.2 ppm is assigned to the ^{11}B sites in $KSc(BH_4)_4$. Only one resonance is observed for the three distinct ^{11}B sites in the $KSc(BH_4)_4$ structure, which reflects that the chemical environments of the boron sites are very similar. This is clearly the case for B1 and B2, which exhibit the same coordination in the second coordination sphere to one Sc and one K. The significant line broadening (0.8 ppm increase in fwhm), caused by acquisition of the spectrum without ^{1}H decoupling (Figure 6b) for both the $KSc(BH_4)_4$ and KBH_4 resonances, demonstrates that boron has

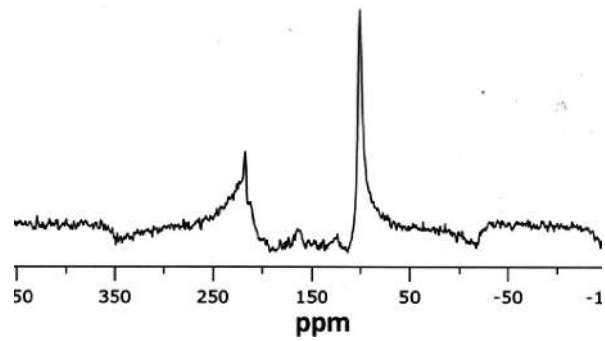

Figure 7. ^{45}Sc MAS NMR of the ball milled KBH_4-ScCl_3 (2:1) sample.

hydrogen in its nearest vicinity, i.e., BH_4 units in accordance with the refined structure by SR-PXD. The observed ^{11}B chemical shift for $KSc(BH_4)_4$ is similar to those previously reported for $LiSc(BH_4)_4$ (^{11}B, −23.0 ppm) and $NaSc(BH_4)_4$ (^{11}B, −21.6 ppm).[24,25]

The MAS ^{45}Sc NMR spectrum (Figure 7) contains signals at 218 and 103 ppm for K_3ScCl_6 and $KSc(BH_4)_4$, respectively. These resonances compare closely to the chemical shifts observed for $LiSc(BH_4)_4$ (113 ppm), $NaSc(BH_4)_4$ (115 ppm), and Na_3ScCl_6 (219 ppm). However, it is noted that the resonance for the potassium salt of $[Sc(BH_4)_4]^-$ anion is significantly less deshielded than those of the lithium and sodium salts. This observation is in accordance with the loser ion pairing in the case of the large potassium ion.

Thermal Analysis. The results from TGA and DSC analysis for all samples are displayed in Figure 8. In all cases, the alkali halide KCl was identified by PXD in the residue after the thermal analysis experiments.

In general, the TGA and DSC data for all three $KSc(BH_4)_4$ samples exhibit the same characteristics. The mass loss occurs in two rapid steps between approximately 460−500 and 510−590 K. Small endothermic peaks are observed in the DSC data at 414, 422, 490, and ∼527 K (peak values). The first two peaks are not related to a mass loss, i.e., the peaks correspond to melting as discussed later. The latter two DSC thermal events proceed over relatively wide temperature intervals of 470−500 and 510−580 K and correspond well with the two observed ranges for the mass loss (DSC peak values and enthalpies for all three samples are listed in Table S5 of the Supporting Information).

The observed total mass loss for the three samples is 1.44, 1.94, and 2.32 wt %, while the calculated hydrogen contents in the samples are 3.11, 3.86, and 4.39 wt % for the KBH_4-ScCl_3 mixtures 2:1, 3:1, and 4:1, respectively (see Table 1). A short exposure of the samples to air during transfer to the TGA-DSC instrument might cause a fraction of the sample to oxidize, prior to the TGA experiment. However, the fact that the observed mass losses are smaller than the calculated hydrogen contents in the samples indicates that the mass loss probably corresponds to release of hydrogen gas only (no diborane); hence, a major fraction or all boron remains in the solid dehydrogenated sample.

The first observed mass loss in the temperature range 460−500 K corresponds to the decomposition of $KSc(BH_4)_4$ and is similar for the 2:1 and 3:1 samples, i.e., 0.71 and 0.82 wt %, respectively, however, only 0.53 wt % for the 4:1 sample. The second mass loss in the range 510−580 K increases significantly as the amount of KBH_4 in the samples increases, being 0.73, 1.12, and 1.79 wt % for the 2:1, 3:1, and 4:1 samples, respectively. This coincides with that smaller amounts of the

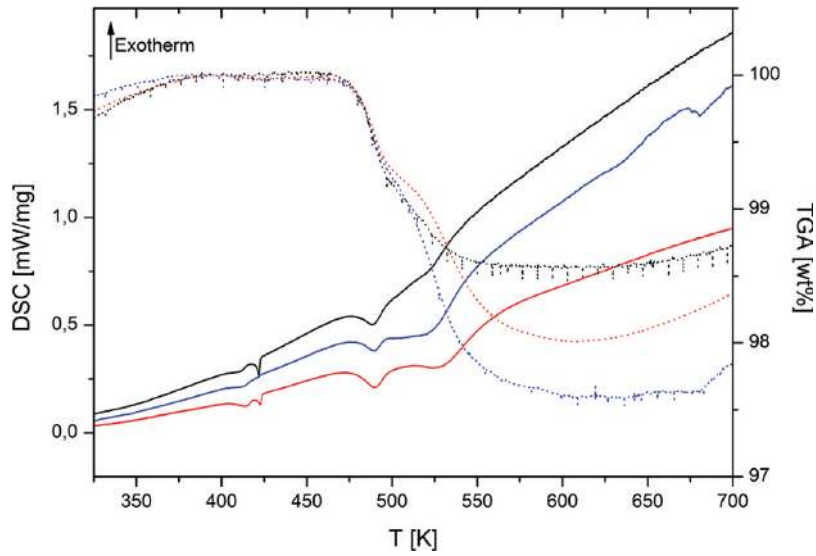

Figure 8. TGA-DSC data for the samples containing $KSc(BH_4)_4$ and K_3ScCl_6. Solid lines, DSC; dashed lines, TGA; black lines, KBH_4-ScCl_3 mixture ratio 2:1; red lines, 3:1; blue lines, 4:1.

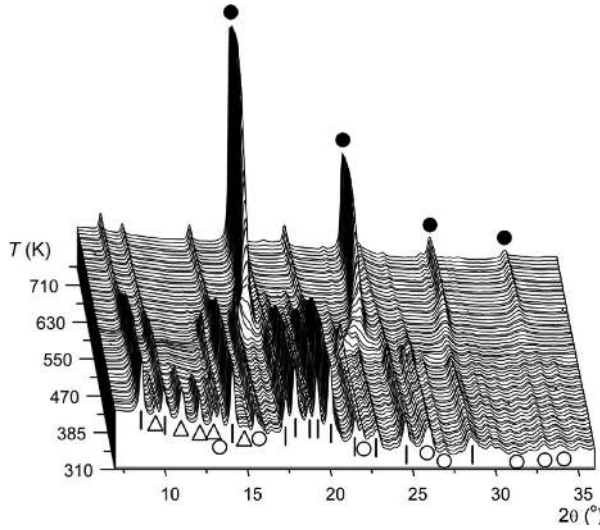

Figure 9. In situ synchrotron radiation powder X-ray diffraction measured for the KBH_4-ScCl_3 mixture 2:1 heated from RT to 773 K with a heating rate of 7 K/min and $p(H_2) \sim 2.5$ bar ($\lambda = 0.9077$ Å). Only peaks which are at least partly resolved are marked by the symbols: △ $KSc(BH_4)_4$, | K_3ScCl_6, ○ KBH_4, and ● KCl.

hydrogen within the sample is in $KSc(BH_4)_4$ as the amount of KBH_4 in the starting composition is increased.

Decomposition Analysis by in Situ SR-PXD. Figure 9 shows *in situ* SR-PXD data for the ball milled mixture KBH_4-ScCl_3 2:1 in the temperature range 310−750 K, and the first PXD patterns reveal the presence of the three compounds $KSc(BH_4)_4$, K_3ScCl_6, and KBH_4. The diffraction peaks corresponding to $KSc(BH_4)_4$ disappear at ∼405 K likely due to melting in accordance with an endothermic DSC peak (at 414 K) and no TGA mass loss. An increase in the diffracted intensity from KBH_4 is observed between ∼460 and 510 K simultaneously with a TGA mass loss. Rietveld refinement of the SR-PXD data measured at 420 K, i.e., after the melting but prior to the decomposition of $KSc(BH_4)_4$, shows the sample contains 9 wt % KBH_4, whereas refinement of the data measured at 505 K, which is after the decomposition of $KSc(BH_4)_4$, reveals that the KBH_4 content has increased to 23 wt %. This observation suggests decomposition of molten $KSc(BH_4)_4$ to KBH_4 and possibly amorphous scandium borides, boron, and/or "higher" boranes with a lower hydrogen content. The decomposition reaction may involve several steps and possibly intermediate phases, which needs further investigation.

Diffraction peaks from K_3ScCl_6 begin to decrease at ∼500 K; meanwhile, the position of the KBH_4 peaks changes position toward higher 2θ values; i.e., the unit cell volume is decreasing. This suggests that two simultaneous and coupled reactions take place. The ternary chloride K_3ScCl_6 reacts with KBH_4, which produces potassium chloride, KCl, and possibly also amorphous scandium borides, boron, and/or "higher" boranes. Simultaneously, the formed KCl dissolves in the remaining KBH_4 and forms a solid solution of composition $K(BH_4)_{1-x}Cl_x$; see reaction scheme 2.

$$x\mathrm{KCl(s)} + (1 - x)\mathrm{KBH_4(s)} \rightarrow \mathrm{K(BH_4)_{1-x}Cl_x(s)} \quad (2)$$

As more KBH_4 is consumed and more KCl is formed during the reaction with K_3ScCl_6, the degree of substitution x increases. The reaction between KBH_4 and K_3ScCl_6 observed by in situ SR-PXD corresponds well with the mass loss and thermal events observed in TGA and DSC between 510 and 590 K. Formation of a solid solution was also observed recently during decomposition of $NaSc(BH_4)_4$.[25] Furthermore, fast dissolution (within minutes) of LiCl in $LiBH_4$ was observed at 383 K < T < 523 K and relatively slow segregation of LiCl from the solid solution $Li(BH_4)_{1-x}Cl_x$ at RT.[45,46]

The dissolution of potassium chloride in potassium borohydride was investigated in further detail by Rietveld refinement of the *in situ* SR-PXD data for the 4:1 sample, which contains the highest amount of KBH_4. A structural model was developed where a Cl substitute for BH_4, i.e., Cl was constrained to the same set of x,y,z coordinates as B, and the sum of their occupancies was constrained to 1. Figure 10 shows the change in the unit cell parameter (left) and in the substitution degree, x, in $K(BH_4)_{1-x}Cl_x$ (right) as a function of temperature. From RT to ∼500 K, no substitution in KBH_4 is observed, i.e., $x = 0$. This indicates that no KCl is formed during ball milling, as suggested by reaction 1. At ∼500 K, the unit cell parameter begins to decrease; meanwhile, x increases. At ∼610 K, a plateau is reached where $a \sim 6.52$ Å and $x \sim 0.78$. Upon further heating at ∼730 K, the substitution continues likely due to slow

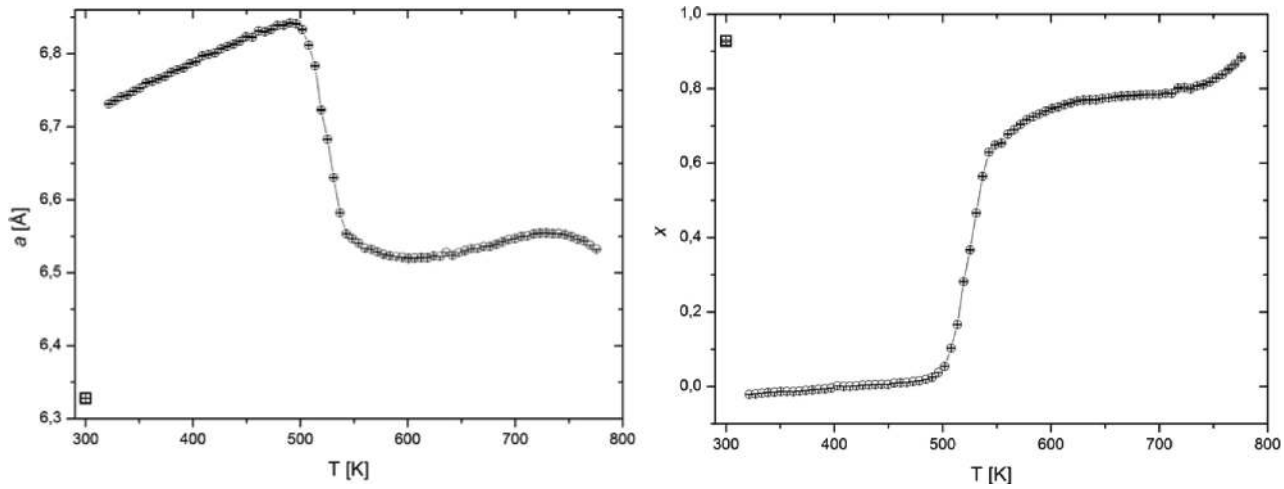

Figure 10. Cell parameter a (left) and substitution degree x (right) for $K(BH_4)_{1-x}Cl_x$ obtained from Rietveld refinement of in situ SR-PXD data of a ball milled KBH_4-ScCl_3 (4:1) sample. Symbols: ○ values during heating, □ values after heating/cooling.

decomposition of the KBH_4 contained in the $K(BH_4)_{1-x}Cl_x$ solid solution. As the sample is cooled to RT, a final unit cell parameter of $a = 6.3278(7)$ Å is obtained, which corresponds to an overall decrease of 6% and a change in composition from KBH_4 to the solid solution $K(BH_4)_{0.07}Cl_{0.93}$ formed at RT after the *in situ* SR-PXD experiment.

For the samples containing a smaller amount of KBH_4 (samples 2:1 and 3:1), separate diffraction from KCl appears at ~540 K, suggesting that the amount of KBH_4 in these samples is too small to accommodate all KCl formed by the reaction of the ternary chloride K_3ScCl_6 with KBH_4. This further indicates that KCl is formed separately by this reaction prior to formation of the solid solution $K(BH_4)_{1-x}Cl_x$ (2).

In the 2:1 sample, not all K_3ScCl_6 is consumed by the reaction with KBH_4 and between 625 and 769 K a new high temperature cubic polymorph of K_3ScCl_6 ($a = 10.694$ Å at 769 K) is observed, which is isostructural to HT-K_3YCl_6[47] (cubic structure type $[NH_4]_3FeF_6$, *Fm*3*m*, perovskite superstructure). The same cubic structure type has been observed at RT for Cs_2KScCl_6.[48]

The thermal decomposition of $KSc(BH_4)_4$ and hydrogen release are very similar to what has been observed for $NaSc(BH_4)_4$.[25] In both cases, one of the starting products of the synthesis, the alkali metal borohydride, is formed in the first step of hydrogen release. Then, the ternary alkaline scandium chloride formed during the initial synthesis plays a positive role and is involved in the second step of the reaction of hydrogen release. The melting temperature of the alkaline scandium borohydride and temperatures of the two hydrogen release steps are very similar for both alkali metals, K and Na. In contrast, no ternary chloride is formed during the synthesis of $LiSc(BH_4)_4$ from $LiBH_4$ and $ScCl_3$, even though Li_3ScCl_6 exists.[49] Between 390 and 412 K, $LiSc(BH_4)_4$ decomposes to $LiBH_4$ and an amorphous decomposition product[50] (see Figure S2, Supporting Information) similar to the formation of KBH_4 during decomposition of $KSc(BH_4)_4$. $LiBH_4$ then reacts with LiCl and forms $Li(BH_4)_{1-x}Cl_x$ solid solution. The amorphous products have later been identified as ScB_2, B, and $Li_2B_{12}H_{12}$.[51] To release all hydrogen from the sample, heating up to 623 K is needed.[51]

Thermal Expansion. The thermal behavior of the $KSc(BH_4)_4$ lattice parameters is slightly nonlinear, as illustrated in Figures 11 and 12. The volumetric thermal expansion coefficient can be linearly approximated in the interval 295−360 K (Figure 11) as $\alpha_V = 3.21(1) \times 10^{-4}$ K^{-1}, slightly bigger than that of $NaSc(BH_4)_4$ ($\alpha_V = 2.54(3) \times 10^{-4}$ K^{-1})[25] and of $LiSc(BH_4)_4$

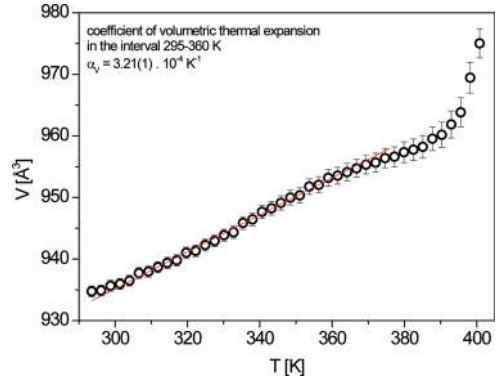

Figure 11. Cell volume of $KSc(BH_4)_4$ as a function of temperature.

($\alpha_V = 1.46(1) \times 10^{-4}$ K^{-1}); see Figure S3 of the Supporting Information.[50] The *b*-lattice parameter of $KSc(BH_4)_4$ shows strong nonlinearity close to the melting temperature (Figure 12). The thermal behavior of the K_3ScCl_6 lattice parameters in the interval 295−360 K is given in the Supporting Information as Figures S4 and S5. Thermal expansion of the HT-polymorph of K_3ScCl_6 was not possible to evaluate due to decreasing content of K_3ScCl_6 in the sample consumed by the reaction with KBH_4.

Relation to Other Structures. $KSc(BH_4)_4$ is a new example of a growing family of alkali metal or alkaline-earth metal−transition metal borohydrides with the general formula $A^{m+}M^{n+}(BH_4)_{m+n}$ whose crystal structure is described. Several compounds within this class of materials were reported in the literature with the tentative compositions $LiZn(BH_4)_3$, $Li_2Zn(BH_4)_4$, $NaZn(BH_4)_3$, $BaZn_3(BH_4)_8$,[52] and $K_2Zn_3(BH_4)_8$,[53,54] and the crystals structures of $LiSc(BH_4)_4$,[24] $NaSc(BH_4)_4$,[25] $LiZn_2(BH_4)_5$, $NaZn_2(BH_4)_5$, $NaZn(BH_4)_3$,[41] $KZn(BH_4)Cl_2$,[38] and $Li_4Al_3(BH_4)_{13}$[10] have been recently determined.

In all three scandium-based compounds, $LiSc(BH_4)_4$, $NaSc(BH_4)_4$, and $KSc(BH_4)_4$, the $[Sc(BH_4)_4]^-$ anion is located inside alkaline-metal cages (Figure 13): slightly deformed trigonal Na_6 prisms (each second prism empty) in $NaSc(BH_4)_4$ (triangular angles 55.5 and 69.1°), tetragonal Li_8 prisms (all prisms occupied) in $LiSc(BH_4)_4$, and side monocapped trigonal prisms K_7 (all prisms occupied) in $KSc(BH_4)_4$ (triangular angles 53.3 and 73.4°). Please note that the Li position is disordered along the *c*-axis in $LiSc(BH_4)_4$[24] and therefore the exact shape of the Li_8 polyhedra remains to be determined. The disordered lithium atom in $LiSc(BH_4)_4$ apparently has a linear coordination

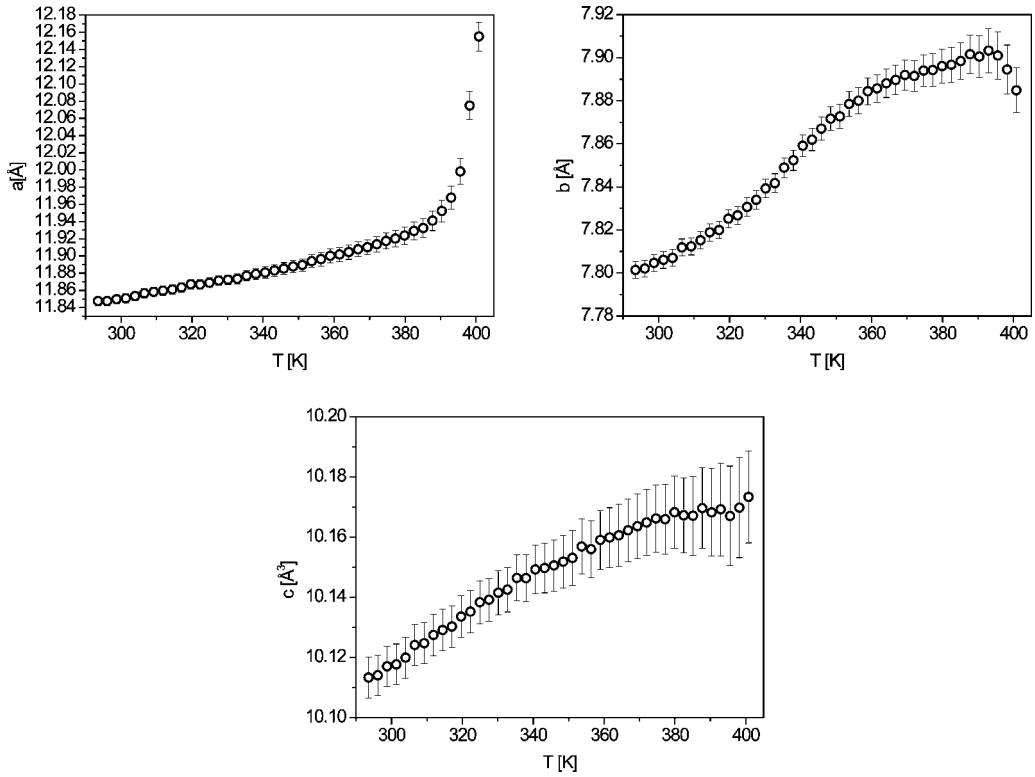

Figure 12. Lattice parameters of $KSc(BH_4)_4$ as a function of temperature.

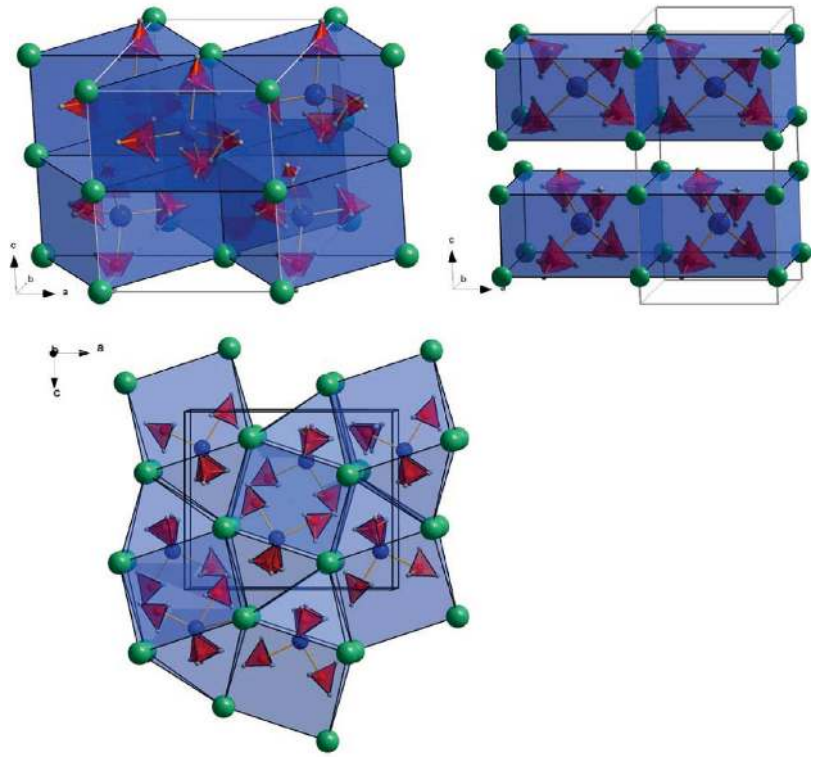

Figure 13. Crystal structure of $NaSc(BH_4)_4$ (top left), of $LiSc(BH_4)_4$ (top right), and of $KSc(BH_4)_4$ (bottom left) viewed approximately along the *b*-axes showing the coordination of Sc atoms (blue) by BH_4 tetrahedra (red). The $[Sc(BH_4)_4]^-$ anions are located inside slightly deformed trigonal prisms Na_6 (each second prism empty) in $NaSc(BH_4)_4$ (triangular angles 55.5 and 69.1°), inside tetragonal prisms Li_8 (all prisms occupied) in $LiSc(BH_4)_4$, and inside side monocapped trigonal prisms K_7 (all prisms occupied) in $KSc(BH_4)_4$ (triangular angles 53.3 and 73.5°). The Li position is disordered along the *c*-axis in $LiSc(BH_4)_4$. The packing of Na^+ cations and $[Sc(BH_4)_4]^-$ anions in $NaSc(BH_4)_4$ corresponds to a distorted variant of the hexagonal NiAs structure type, and the packing of K^+ cations and $[Sc(BH_4)_4]^-$ anions in $KSc(BH_4)_4$ corresponds to the orthorhombic Np metal structure type.

by two BH_4 groups,[24] while the coordination number of sodium in $NaSc(BH_4)_4$ is 6,[25] and that of potassium in $KSc(BH_4)_4$ is 8. The increase of the coordination number for alkali metal atoms in scandium-based borohydrides correlates with the increase of their atomic radii. The coordination numbers for the borohydride anions increase accordingly in the series, from Li to K.

The structure of $KSc(BH_4)_4$ is of the $BaSO_4$ type where the BH_4 tetrahedra are on the positions of oxygen atoms. This structure type has been previously found in borohydrides only once, in the high-pressure phase of $NaBH_4$.[55] Regarding the packing of K^+ cations and $[Sc(BH_4)_4]^-$ anions in $KSc(BH_4)_4$, the structure can be seen as a distorted variant of the orthorhombic Np metal structure type[56] (Figure 13). As the Np metal structure type is derived from the bcc structure, it shows that the primary building principle in $KSc(BH_4)_4$ is the packing of K^+ cations and $[Sc(BH_4)_4]^-$ anions. Similar analogies can be drawn also for $NaSc(BH_4)_4$: its structure resembles $CrVO_4$ (ref 57, own structure type) where the BH_4 tetrahedra are on the positions of oxygen atoms, and the packing of units can be considered as an ordered binary variant of the hcp structure. The complex anion $[Al(BH_4)_4]^-$ and the complex cation $[(BH_4)Li_4]^{3+}$ in $Li_4Al_3(BH_4)_{13}$[10] are also closely packed in the structure type Cr_3Si (A15), a Frank−Kasper phase with 14- and 12-coordinated sites. The above analysis shows that the alkali metal−scandium borohydrides are built by packing of discrete $[Sc(BH_4)_4]^-$ anions and alkali metal cations. The packing varies and the coordination numbers of cations increase as the ionic radius of the alkali metal increases from Li to K.

Conclusions

$KSc(BH_4)_4$ is a new example of an alkali metal-transition metal borohydride whose crystal structure is described. The new compound has been studied by using a combination of *in situ* synchrotron powder diffraction, thermal analysis, and MAS NMR, Raman, and infrared spectroscopy. The structure of $KSc(BH_4)_4$ consists of isolated $[Sc(BH_4)_4]^-$ anions located inside slightly deformed side monocapped trigonal prisms K_7. The experimental results show that each Sc^{3+} is tetrahedrally surrounded by four BH_4 tetrahedra with a 12-fold coordination to hydrogen. Compared to $LiSc(BH_4)_4$, the $[Sc(BH_4)_4]^-$ anion in $KSc(BH_4)_4$ is less deformed but more deformed than in $NaSc(BH_4)_4$. The packing of K^+ cations and $[Sc(BH_4)_4]^-$ anions in the structure of $KSc(BH_4)_4$ forms a distorted variant of the orthorhombic Np metal structure type showing packing of cations and anions as a primary structural building principle.

A new ternary chloride K_3ScCl_6, isostructural to K_3MoCl_6, was identified as a second phase in all samples. This indicates that the formation of $KSc(BH_4)_4$ during ball milling of KBH_4 and $ScCl_3$ is a complex reaction, which may involve formation of KCl as an intermediate phase. It resembles the reaction between $NaBH_4$ and $ScCl_3$ where the ternary chloride forms too, and differs from the reaction between $LiBH_4$ and $ScCl_3$ forming binary LiCl.

$KSc(BH_4)_4$ is stable from RT up to ∼405 K, where the compound melts and then releases hydrogen in two rapid steps between approximately 460−500 and 510−590 K. The hydrogen release involves the formation of KBH_4, its reaction with K_3ScCl_6, and formation of $K(BH_4)_{1-x}Cl_x$ solid solution. The nonreacted K_3ScCl_6 transforms at 635 K to a cubic polymorph isostructural to the high temperature phase of K_3ScCl_6. The decomposition of $KSc(BH_4)_4$ is similar to that of $NaSc(BH_4)_4$.

Preparation of bimetallic alkaline (Li, Na, and K) transition metal (Sc) borohydrides allows the hydrogen desorption temperature of the stable alkali metal borohydrides to be decreased.

Acknowledgment. G.S. and C.M.J. acknowledge the financial support of the Office of Hydrogen Fuel Cells and Infrastructure Technology of the U.S. Department of Energy for their portion of this work. T.R.J. and D.B.R. thank the Danish Research Council for Nature and Universe (Danscatt), the Danish National Research Foundation (Centre for Materials Crystallography), the Danish Strategic Research Council (Centre for Energy Materials), and the Carlsberg Foundation for funding. This work was supported by the Swiss National Science Foundation. The authors acknowledge SNBL and MAX-lab for the beamtime allocation.

Supporting Information Available: Table of atomic positions; representative Rietveld refinement profile; crystal data as CIF file. This material is available free of charge via the Internet at http://pubs.acs.org.

References and Notes

(1) Soloveichik, G. *Mater. Matters (Milwaukee, WI, U. S.)* **2007**, *2*, 11–14.
(2) Orimo, S.; Nakamori, Y.; Eliseo, J. R.; Züttel, A.; Jensen, C. M. *Chem. Rev.* **2007**, *107*, 4111–4132.
(3) Grochala, W.; Edwards, P. P. *Chem. Rev.* **2004**, *104*, 1283–1315.
(4) Mauron, P.; Buchter, F.; Friedrichs, O.; Remhof, A.; Bielmann, M.; Zwicky, C. N.; Züttel, A. Stability and Reversibility of LiBH4. *J. Phys. Chem. B* **2008**, *112*, 906–910.
(5) Vajo, J. J.; Skeith, L. S.; Mertens, F. *J. Phys. Chem. B* **2005**, *109*, 3719–3722.
(6) Bösenberg, U.; Doppiu, D.; Mosegaard, L.; Barkhordarian, G.; Eigen, N.; Borgschulte, A.; Jensen, T. R.; Cerenius, Y.; Gutfleisch, O.; Klassen, T.; et al. *Acta Mater.* **2007**, *55*, 3951–3958.
(7) Pinkerton, F. E.; Meyer, M. S.; Meisner, G. P.; Balogh, M. P.; Vajo, J. J. *J. Phys. Chem. C* **2007**, *111*, 12881–12885.
(8) Walker, G. S.; Grant, D. M.; Price, T. C.; Yu, X.; Legrand, L. *J. Power Sources* **2009**, *194*, 1128–1134.
(9) Lee, J. Y.; Ravnsbæk, D.; Cerenius, Y.; Kim, Y.; Lee, Y.-S.; Shim, J.-H.; Jensen, T. R.; Cho, Y. W. *J. Phys. Chem. C* **2009**, *113*, 15080–15086.
(10) Lindemann, I.; Domènech Ferrer, R.; Dunsch, L.; Filinchuk, Y.; Černý, R.; Hagemann, H.; D'Anna, V.; Lawson Daku, L. M.; Schultz, L.; Gutfleisch, O. *Chem.—Eur. J.* **2010**, *16*, 8707–8712.
(11) Schrauzer, G. N. *Naturwissenschaften* **1995**, *42*, 438.
(12) Sanderson, R. T. *Science* **1951**, *114*, 670–672.
(13) Nakamori, Y.; Miwa, K.; Ninomiya, A.; Li, H.-W.; Ohba, N.; Towata, S.; Züttel, A.; Orimo, S. *Phys. Rev. B* **2006**, *74*, 045126.
(14) Jensen, C. M.; Sulic, M.; Kuba, M.; Brown, C.; Langley, W.; Dalton, T.; Culnane, L.; Severa, G.; Eliseo, J.; Ayabe, R.; Zhang, S. *Proceedings of the U.S. DOE Hydrogen and Fuel Cells Annual Program/ Lab R&D Review*, Arlington, VA, May 14−18, 2007.
(15) Li, H.-W.; Orimo, S.; Nakamori, Y.; Miwa, K.; Ohba, N.; Towata, S.; Züttel, A. *J. Alloys Compd.* **2007**, *446−447*, 315–318.
(16) Filinchuk, Y.; Chernyshov, D.; Dmitriev, V. *Z. Kristallogr.* **2008**, *223*, 649–659; the 2010 update in arXiv:1003.5378.
(17) Bird, P. H.; Churchill, M. R. *Chem. Commun.* **1967**, 403–405.
(18) Broach, R. W.; Chuang, I. S.; Marks, T. J.; Williams, J. M. *Inorg. Chem.* **1983**, *22*, 1081–1084.
(19) Haaland, A.; Shorokhov, D. J.; Tutukin, A. V.; Volden, H. V.; Swang, O.; Sean McGrady, G.; Kaltsoyannis, N.; Downs, A. J.; Tang, Ch. Y.; Turner, J. F. C. *Inorg. Chem.* **2002**, *41*, 6646–6655.
(20) Sato, T.; Miwa, K.; Nakamori, Y.; Ohoyama, K.; Li, H.-W.; Noritake, T.; Aoki, M.; Towata, S.-I.; Orimo, S.-I. *Phys. Rev. B* **2008**, *77*, 104114.
(21) Jaron, T.; Grochala, W. *Dalton Trans.* **2010**, *39*, 160–166.
(22) Ravnsbæk, D.; Filinchuk, Y.; Černý, R.; Ley, M. B.; Haase, D.; Jakobsen, H. J.; Skibsted, J.; Jensen, T. R. *Inorg. Chem.* **2010**, *49*, 3801–3809.
(23) Frommen, C.; Aliouane, N.; Deledda, S.; Fonneløp, J. E.; Grove, H.; Lieutenant, K.; Llamas-Jansa, I.; Sartori, S.; Sørby, M. H.; Hauback, B. C. *J. Alloys Compd.* **2010**, *496*, 710–716.
(24) Hagemann, H.; Longhini, M.; Kaminski, J. W.; Wesolowski, T. A.; Černý, R.; Penin, N.; Sorby, M. H.; Hauback, B. C.; Severa, G.; Jensen, C. M. *J. Phys. Chem. A* **2008**, *112*, 7551–7555.
(25) Černý, R.; Severa, G.; Ravnsbæk, D.; Filinchuk, Y.; D'Anna, V.; Hagemann, H.; Haase, D.; Jensen, C. M.; Jensen, T. R. *J. Phys. Chem. C* **2010**, *114*, 1357–1364.
(26) Mammen, C. B.; Ursby, T.; Cerenius, Y.; Thunnissen, M.; Als-Nielsen, J.; Larsen, S.; Liljas, A. *Acta Phys. Pol., A* **2002**, *101*, 595–602.
(27) Clausen, B. S.; Steffensen, G.; Fabius, B.; Villadsen, J.; Feidenhans'l, R.; Topsøe, H. *J. Catal.* **1991**, *132*, 524–535.
(28) Jensen, T. R.; Nielsen, T. K.; Filinchuk, Y.; Jørgensen, J. E.; Cerenius, Y.; Gray, E.MacA.; Webb, C. J. *J. Appl. Crystallogr.*, in press, **2010**. DOI: 10.1107/S0021889810038148.
(29) Hammersley, A. P.; Svensson, S. O.; Hanfland, M.; Fitch, A. N.; Häusermann, D. *High Pressure Res.* **1996**, *14*, 235–248.
(30) Boultif, A.; Louer, D. *J. Appl. Crystallogr.* **2004**, *37*, 724–731.

(31) Favre-Nicolin, V.; Černý, R. *J. Appl. Crystallogr.* **2002**, *35*, 734–743.
(32) Coelho, A. A. TOPAS-Academic; http://members.optusnet.com.au/~alancoelho.
(33) Spek, A. L. *PLATON*; University of Utrecht: The Netherlands, 2006.
(34) Efron, B.; Tibshirani, R. *Stat. Sci.* **1986**, *1*, 54–77.
(35) Amilius, Z.; Van Laar, B.; Rietveld, H. M. *Acta Crystallogr., Sect. B* **1969**, *25*, 400–402.
(36) Filinchuk, Y.; Černý, R.; Hagemann, H. *Chem. Mater.* **2009**, *21*, 925–933.
(37) Filinchuk, Y.; Hagemann, H. *Eur. J. Inorg. Chem.* **2008**, 3127–3133.
(38) Ravnsbæk, D.; Sørensen, L. H.; Filinchuk, Y.; Reed, D.; Book, D.; Cerenius, Y.; Jakobsen, H. J.; Besenbacher, F.; Skibsted, J.; Jensen, T. R. *Eur. J. Inorg. Chem.* **2010**, 1608–1612.
(39) Soulié, J.-P.; Renaudin, G.; Černý, R.; Yvon, K. *J. Alloys Compd.* **2002**, *346*, 200–205.
(40) Filinchuk, Y.; Chernyshov, D.; Černý, R. *J. Phys. Chem. C* **2008**, *112*, 10579–10584.
(41) Ravnsbæk, D.; Filinchuk, Y.; Cerenius, Y.; Jakobsen, H. J.; Besenbacher, F.; Skibsted, J.; Jensen, T. R. *Angew. Chem., Int. Ed.* **2009**, *48*, 6659–6663.
(42) Marks, T. J.; Kolb, J. R. *Chem. Rev.* **1977**, *77*, 263.
(43) Smith, B. E.; Schurvell, H. F.; James, B. D. *J. Chem. Soc., Dalton Trans* **1977**, 710.
(44) Keiderling, T. A.; Wozniak, W. T.; Gay, R. S.; Jurkowitz, D.; Bernstein, E. R.; Lippard, S. J.; Spiro, T. G. *Inorg. Chem.* **1975**, *14*, 576.
(45) Mosegaard, L.; Møller, B.; Jørgensen, J.-E.; Filinchuk, Y.; Cerenius, Y.; Hanson, J.; Dimasi, E.; Besenbacher, F.; Jensen, T. *J. Phys. Chem. C* **2008**, *112*, 1299–1303.
(46) Arnbjerg, L. M.; Ravnsbæk, D.; Filinchuk, Y.; Vang, R. T.; Cerenius, Y.; Besenbacher, F.; Jørgensen, J.-E.; Jacobsen, H. J.; Jensen, T. R. *Chem. Mater.* **2009**, *21*, 5772–5782.
(47) Mattfeld, H.; Meyer, G. *Z. Anorg. Allg. Chem.* **1992**, *618*, 13–17.
(48) Meyer, G.; Hwu, S. J.; Corbett, J. D. *Z. Anorg. Allg. Chem.* **1986**, *535*, 208–212.
(49) Bohnsack, A.; Stenzel, F.; Zajonc, A.; Balzer, G.; Wickleder, M. S.; Meyer, G. *Z. Anorg. Allg. Chem.* **1997**, *623*, 1067–1073.
(50) Černý, R.; Hagemann, H.; Filinchuk, Y. Unpublished results.
(51) Kim, Ch.; Hwang, S. J.; Bowman, R. C., Jr.; Reiter, J. W.; Zan, J. A.; Kulleck, J. G.; Kabbour, H.; Majzoub, E. H.; Ozolins, V. *J. Phys. Chem. C* **2009**, *113*, 9956–9968.
(52) Nöth, H.; Wiberg, E.; Winter, L. P. *Z. Anorg. Allg. Chem.* **1971**, *386*, 73–86.
(53) Hagenmuller, P.; Rault, M. *C. R. Acad. Sci.* **1959**, *248*, 2758–2760.
(54) Mal'tseva, N. N.; Sheiko, O. V.; Bakulina, V. M.; Mikheeva, V. I. *Russ. J. Inorg. Chem.* **1970**, *15*, 363–364.
(55) Filinchuk, Y.; Talyzin, A. V.; Chernyshov, D.; Dmitriev, V. *Phys. Rev. B* **2007**, *76*, 092104.
(56) Zachariasen, W. H. *Acta Crystallogr.* **1952**, *5*, 660–664.
(57) Frazer, B. C.; Brown, P. J. *Phys. Rev.* **1962**, *125*, 1283–1291.

JP106280V